A Model for Astral Stimulation of Cytokinesis in Animal Cells

John J. Devore,* Gary W. Conrad,‡§ and Raymond Rappaport§‖

* Department of Electrical and Computer Engineering and ‡ Division of Biology, Kansas State University, Manhattan, Kansas 66506; § Mount Desert Island Biological Laboratory, Salsbury Cove, Maine 04672; and ‖ Department of Biological Sciences, Union College, Schenectady, New York 12308

Abstract. A model is proposed in which stimulation of cortical cytoplasm occurs near the distal ends of astral rays. Levels of stimulation sufficient to cause furrowing occur only in equatorial zones between asters. The model can account for positioning of furrows in very large cells (fertilized eggs of amphibians, birds, and fish) and in cells with several mitotic apparatuses (insects). Finally, the model correctly predicts the positioning and occurrence of furrowing in two experiments in which cellular shape was manipulated into either an hourglass or a cylindrical form before division. These results are consistent with equatorial stimulation theories in which mitotic asters differentially stimulate the future furrow region (equatorial cortex). The results are not consistent with models requiring differential stimulation of nonfurrowing, polar regions of the cell.

ECHANISMS by which a mitotic apparatus stimulates cortical cytoplasm of an animal cell to form a cleavage furrow remain a mystery. The apparatus is not necessary mechanically (14, 48). The stimulatory role that it plays requires only a pair of asters since a spindle is not needed (25). The astral pair needs only to interact with the cell surface for ~1 min to accomplish the requisite stimulation (31); a furrow begins to form a few minutes later, even in the absence of the original astral pair (10, 28). Two major theories account for the role of asters in initiation of furrowing. Equatorial stimulation theories propose that a furrow forms wherever two asters overlap (26). Conversely, polar stimulation theories propose that essential activation of cortical cytoplasm occurs at polar regions of spherical cells (4, 45–47). In the accompanying paper by Harris and Gewalt (11), computer simulation methods show that a recent computer model requiring polar signaling (4, 45–47), although capable in principle of generating equatorial furrows in spherical cells, fails to make the correct predictions in experiments where cells have been distorted into other shapes (30).

The computer simulation model described below is based on the equatorial stimulation theory of furrowing and is consistent with natural and experimental furrow formation. The model is based on the following assumptions. First, asters consist of rays that are space filling in length and that approach, but do not actually touch, the cell surface. Second, distribution of astral rays is assumed to be radially symmetric about each astral center, except in solid angles occluded by adjacent astral centers. Third, stimulation of the cortical cytoplasm beneath the cell surface occurs at the ends of the astral rays, reaching levels high enough to elicit a subsequent furrow only where two asters are sufficiently close to overlap

with one another in the region of the cell surface, thus producing a localized region of higher density of ray ends at the cell surface. Fourth, cleavage furrow–stimulating substance is released from the end of each astral ray at a constant rate. Fifth, after its release, stimulating substance undergoes continuous disappearance because of both diffusion and decay; the latter may represent chemical inactivation (e.g., hydrolysis) and/or sequestration (e.g., within a vesicle). Sixth, localized, steady-state concentrations of stimulating substance therefore represent the summed effects of astral ray distributions—continuous substance release from astral ray ends and, simultaneously, continuous disappearance of substance. And, finally, the role of the asters is to stimulate the cell surface to subsequently form a furrow. That is, after the asters have stimulated the cell surface, they could be removed. Their presence is not necessary at the beginning of furrowing per se nor during furrow progression.

The superficial events leading to cytokinesis are relatively simple and can be modeled in several ways based on different assumptions of mechanism. The model of White and Borisy (46) was based on the assumption that reactions essential for subsequent furrow formation occurred at the polar regions of cells. This model provoked useful discussions of possible cleavage mechanisms. However, presentation of an alternative model is now appropriate because the polar stimulation model has been shown to predict incorrectly the effects on cytokinesis of at least fifteen experimental modifications of cellular shape (30, 32). Moreover, a subsequent presentation of the polar stimulation theory (45) acknowledged that a basic and important assumption of the original model was not valid, but the consequences of the changed assumption were not discussed. In the absence of experimental data supporting the polar stimulation model, an alternative model based on equatorial stimulation of furrowing is proposed.

Send correspondence and reprint requests to Dr. Conrad.

2225

Materials and Methods

The computer program was written in C, compiled using the Microsoft C (version 5.1), and run on a personal computer (Z-386; Zenith Data Systems Corp., St. Joseph, MI). The program can be run on any IBM PC-compatible personal computer with 640K memory and a math coprocessor. Figures were generated using GraphiC software (Scientific Endeavors Corp., Kingston, TN) and plotted on a laser printer (LaserJet Series II; Hewlett-Packard Co., Palo Alto, CA) or photographed from a flat screen monitor. A 5 1/4-inch floppy disk containing the program (without GraphiC) can be obtained ($25) via a written purchase order to Cytokinesis Model, Department of Electrical and Computer Engineering, Kansas State University, Manhattan, KS 66506. For questions about the program, contact Dr. John Devore at (913) 532-5600.

The program allows the user to control the cellular shape proposed, the orientation of the mitotic apparatus with respect to the cell surface, the distance between astral centers, the distribution of astral rays, the rate of stimulating substance release from the astral ray ends, and, separately, the rates of substance diffusion and decay. The program specifically makes no assumptions about the molecular weight, ionic form, or chemical nature of the stimulating substance.

Results and Discussion

We postulate that each aster consists of a set of rays from whose distal ends is released a substance that stimulates contractile protein activity in cortical cytoplasm. Below some critical concentrations of substance no furrow forms, whereas above it self-propagating reactions are initiated that become independent of the mitotic apparatus. Contraction of the resulting band of microfilaments in the cortical cytoplasm of the equatorial zone between the asters generates a cleavage furrow. The nature of the stimulatory substance is unknown, but upon release, its localized concentration diminishes with time and distance, both by diffusion and by decay (sequestration or inactivation). The substance is released continuously from distal ends of astral rays, structures that are space filling in length, up to a maximum value determined by the cell perimeter, and that diverge from one another at equal angles. Under these conditions, highest concentrations of substances will occur in the zone where rays of any two asters overlap. This occurs between asters connected by a spindle and where polar regions or lateral regions of unrelated asters overlap. For a pair of asters to cause furrowing requires that a line connecting their centers be parallel with and close to the cell surface (30).

An integral part of our model is a discrete simulation of stimulus movement in a cellular cross section. The simulation is performed using a finite element approach in which the cellular cross section is divided into an array of square elements. Each element contains a stimulus concentration value kept in floating point form. The simulation yields stimulus concentrations for each element at discrete steps in time, thereby generating a discrete-time, discrete-space, continuous-value simulation.

The theory can be modeled adequately in two dimensions by proposing a pair of asters inside a cell, seen in section view, whose plasma membrane and associated cortical cytoplasm are represented as a perimeter line (Fig. 1 a). Each astral ray grows in a straight line until it approaches the perimeter, up to some maximum. At each such ray end (e.g., Fig. 1 a, small circle), stimulatory substance is released continuously. The steady-state concentration of substance released from these ends can be modeled by dividing the section area into an array of small squares and simulating the spread of substance throughout these squares for a sufficient period of time. The simulation is an iterative process where each iteration updates the concentrations for an arbitrary discrete step of time. At each iteration, Fick's law of diffusion (43) is applied to move substance from squares of higher concentration to neighboring squares. When a square is surrounded by lower values, the movement is in eight directions (Fig. 1 b). Distribution to diagonal neighbors is a factor of $1/\sqrt{2}$ less than to neighbors sharing a common side. This reduction helps maintain radial diffusion of stimulus in a square-element array. For the iterative procedure to be stable, the diffusion constant must be such that the concentration in the center square does not become less than any of its neighbors because of movement of substance from it to those neighbors. An iteration in the simulation begins with new substance release in squares containing ray ends. The new substance and substance that had been released during prior iterations spread to neighboring squares of lesser concentrations. Concentration in each square then diminishes by decay. At chosen rates for diffusion and decay, substance concentrations in all squares reach steady-state levels. This can be displayed as a three-dimensional net plot. The steady-state concentration due to a single injection site is shown (Fig. 1 c).

Diffusion causes a sharp percentage decrease in stimulus concentration as one moves away from an injection site: concentration of stimulus 10 units away is only 7% of that at the injection site after 100 iterations. Decay attenuates the signal and guarantees that steady-state concentrations will be reached, placing a limit on the concentrations that will exist at each location within the cell. In living cells, it is likely that both diffusion and decay of the stimulus occur and lead to its very rapid attenuation around each injection site. Thus, for the stimulus to reach a level that will trigger furrowing requires that astral rays terminate near the cortex. Programs therefore were run with both properties functional; maximal diffusion was allowed as defined above. Variations of the decay rate between 0.1 and 5% did not significantly change the shape of the resulting three-dimensional net plot, as expected, but did influence the absolute steady-state concentrations. It also increased the number of iterations (time) required to reach equivalent proximities to those steady-state values. Programs to generate Figs. 1-6 were set at a decay rate of 1% and required an average of 400 iterations to achieve a standard level of 99.5% of the steady-state levels. Each model aster was postulated to contain 360 astral rays, each releasing substance at the same rate.

In our model for stimulation by the mitotic apparatus, the distal end of each astral ray, regardless of length, will be surrounded by a steady-state concentration of stimulus after a period of time. Steady-state concentrations throughout the entire cell will be greatest where the density of astral ray ends is greatest. The model also postulates that astral rays are not likely to penetrate the central region of another aster. Thus, there will be an angle (θ), with respect to the axis between astral centers, below which astral rays are unlikely to reach the cell surface (Fig. 1 a). Presence of this central "shadow" region is required by this model to generate a band of differentially higher stimulation in the equatorial zone of spherical cells (Fig. 2). The greater the shadow, the narrower becomes the zone of equatorial stimulation (Fig. 2) until at ~71° (for the cell diameter and aster placement shown in Fig.
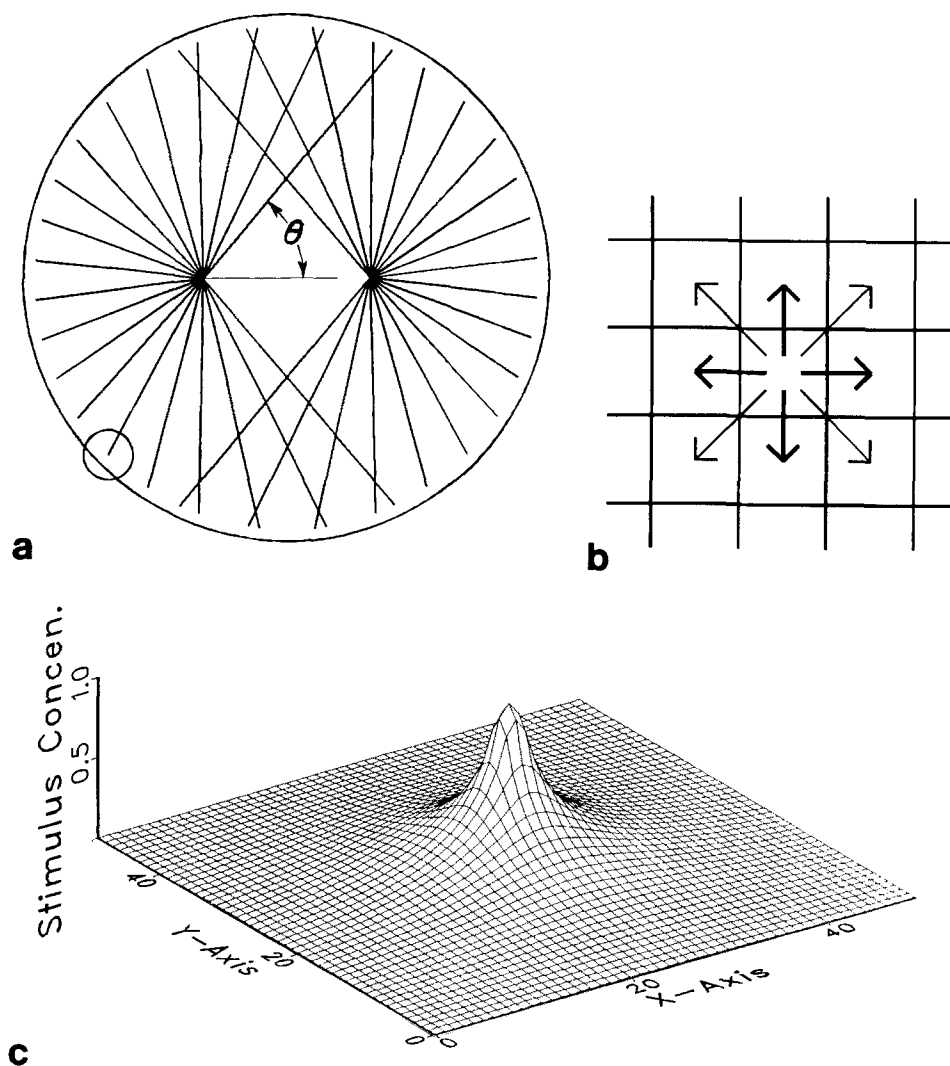
Figure 1. (*a*) Postulated functional two-dimensional distributions of astral rays in a section through a mitotic apparatus within a spherical cell. Rays situated at angle θ or less are excluded (shadow angle) (see text). Stimulatory substance is released continuously from the end of each astral ray (*small circle*) with each iteration of the simulation (time). (*b*) Each such ray end can be modeled as a point source from which the stimulus diffuses to all neighboring regions and simultaneously undergoes loss by decay (sequestration or inactivation). (*c*) A steady-state accumulation of substance thereby forms around the end of each astral ray (stimulus release site), generating steady-state concentrations everywhere in the cell in accord with the distribution of all such astral ray ends (Figs. 2-6).

1) astral rays no longer cross. In the latter case (not shown), concentration of stimulus in the equatorial zone becomes, in fact, slightly less than at the poles. The net plots in Fig. 2 express regional concentrations of stimulus present throughout a two-dimensional section of a spherical cell that passes through the astral centers. The data in Fig. 2 translate into a three-dimensional cell whose entire equator has received more stimulation than either polar zone. This model, therefore, is adequate to explain cytokinesis in a spherical cell.

The model predicts the expected pattern of cell surface stimulation in spherical cells containing a centrally located mitotic apparatus. A furrow will appear symmetrically and simultaneously along the equator encircling the cell. Is a shadow region really present in the mitotic apparatus of such cells? Close examination of fixed mitotic cells, subsequently stained to show the locations of microtubules, does, in fact, suggest the existence of a shadow region from which astral rays are excluded but outside of which astral rays may lengthen and cross near the cortex. Examine, for example, references 36, Fig. 7 *c* (fertilized ascidian egg at anaphase); 37, Fig. 2, *b* and *c* (PtK₁ cells at mid and late anaphase); 39, Fig. 3 *d* and journal cover (sea urchin blastomere at late anaphase); 13, Figs. 20 and 21 (fertilized sea urchin eggs at

anaphase and telophase); 16, Fig. 8, panels *8* and *9* (fertilized *Caenorhabditis elegans* eggs at metaphase and telophase); 8, Fig. 6, *a* and *b* (LLC-PK cell at early anaphase); 38, Fig. 2 *a* (mouse oocytes at meiotic metaphase); 41, Fig. 12 *d* (PtK₁ cell at metaphase); 34, Fig. 11 (newt lung cell at mid prometaphase); and 42, Fig. 2 *g* (fertilized *C. elegans* egg in mitosis). A "cleft of low microtubule density between the central spindle and the aster" has even been noted specifically (reference 34, legend to Fig. 11). The suggestion of a shadow region excluding astral rays also may be seen in living cells (reference 7, Fig. 4 [fertilized sea urchin egg]). After fixation and sectioning, a shadow region also seems evident within the mitotic apparatus (reference 2, Fig. 3, *a* and *b*; 12, Fig. 1, *a* and *b*; and 22, Fig. 1, *c* and *d* [all metaphase and mid anaphase of fertilized sea urchin eggs]). A shadow region seems present between adjacent asters, not always connected by a spindle, in polyploid cells in mitosis and in cells induced to form several asters (reference 13, Fig. 22; and 12, Fig. 5 *b*, [both sea urchin cells]; and 21, Fig. 6 *f*; 41, Fig. 12 *b*; and 1, Fig. 6 [PtK₁ cells]). Finally, asters formed in vitro in cytoplasmic extracts form spindle-like associations with adjacent asters and generate what appears to be a central shadow region (reference 23, Fig. 3 *b*).
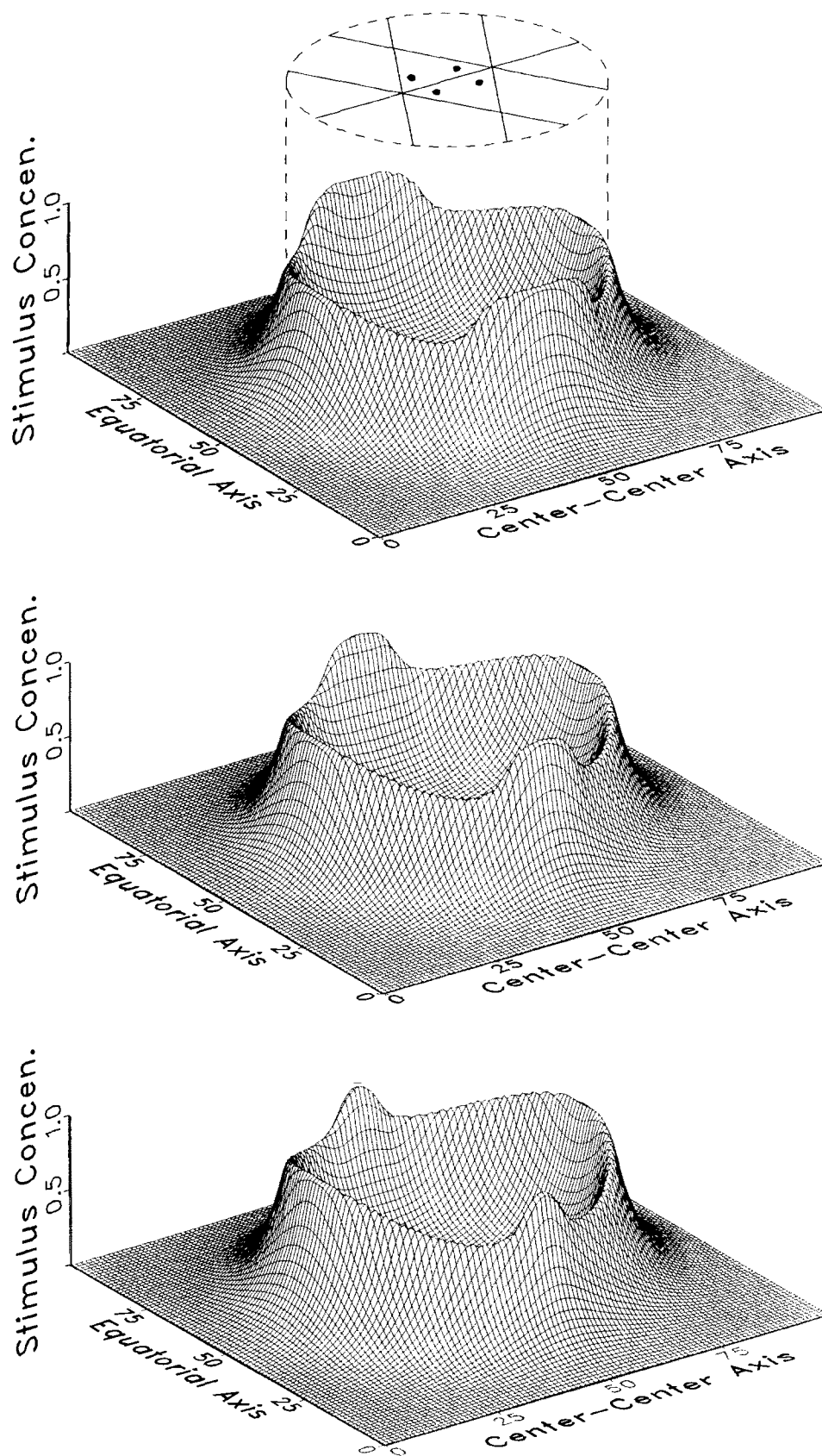
Figure 2. Width of the differential equatorial stimulus band in a spherical cell, as seen in section, becomes progressively narrower as shadow angle θ (*dots*) is increased from 50° (*top*), to 60° (*middle*), and to 65° (*bottom*). Dashed ellipse represents cell perimeter; vertical dashed lines in Figs. 2–6 allow orientation of the cell perimeter with corresponding locations on the net plots.
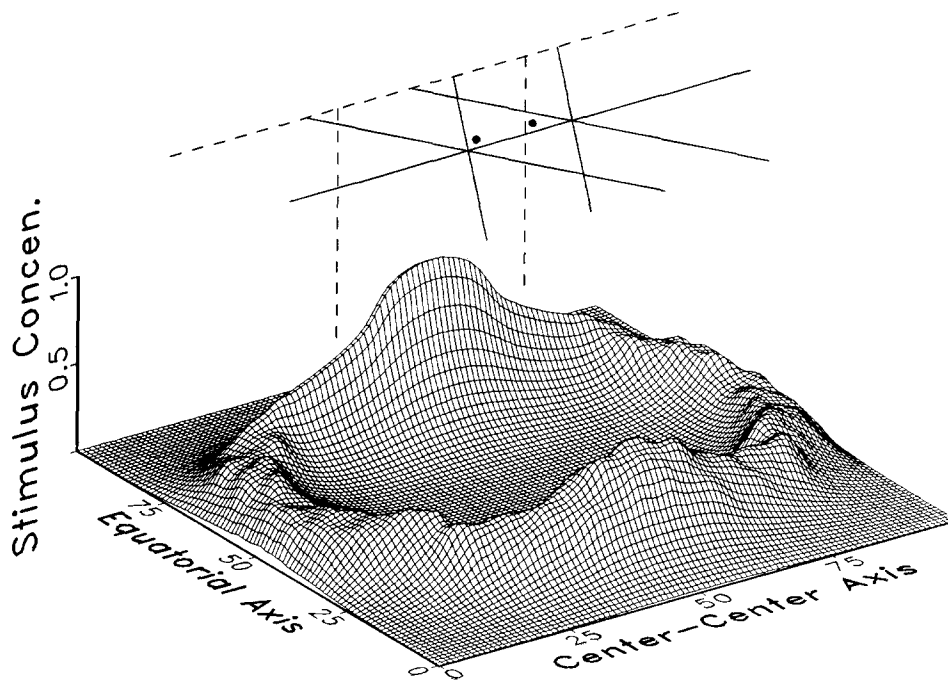
Figure 3. Eccentrically positioned pair of asters stimulates the essentially planar surface, represented as a dashed line parallel to center–center axis, of a fertilized egg of an amphibian, bird, reptile, or fish. Shadow angle (*dots*), 50°.

The shadow region that contains no (or few) astral rays might arise from any tendency of antiparallel arrays of approximately parallel microtubules to form bundles or spindle-like arrays in the cytoplasm (e.g., 23, Fig. 3 *b*). The ability of experimentally formed half-spindles (each with an associated aster) to reassociate and form functional spindles between two asters has been noted previously (40). Those microtubules emanating from a centrosome at slightly too acute an angle to be gathered into such bundles would therefore be situated at angle θ with respect to the spindle axis, as described in Fig. 1. The set of all such microtubules/astral rays would therefore describe the perimeter of the shadow region. Others who have observed such regions of low microtubule density have suggested that "this cleft is most likely formed during spindle assembly as astral microtubules are

incorporated into the central spindle" (34). We know of no data suggesting that an astral ray, emanating from an astral center at an angle less than θ, could penetrate an apposing aster, emerge, and continue lengthening (toward the polar cortex in a spherical cell). Thus, even if antiparallel arrays of microtubules from opposing asters showed no tendency to form bundles, it seems unlikely that astral rays could penetrate the central regions of an apposing astral center. Such blockage alone could create a shadow region between two asters.

The nature of the stimulus emanating from the asters is unknown. Previous experimental manipulations of dividing cells have suggested that, if the stimulus spreads from the asters to the plasma membrane/cortex as a moving front, it does so at ∼6–8 μm/min (27, 29). The rate at which the stim-
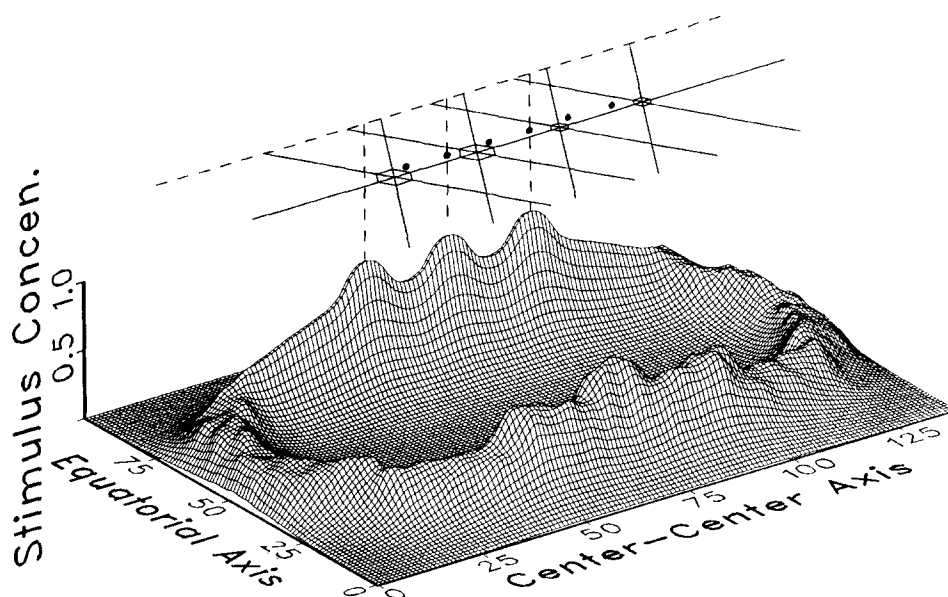

Figure 4. Two pairs of asters abut at their poles, creating an additional zone of furrow stimulation as in the cellularizing blastoderm of *Drosophila* and other insects. The essentially planar surface is represented as a dashed line parallel to the center–center axis. Shadow angle (*dots*), 60°.
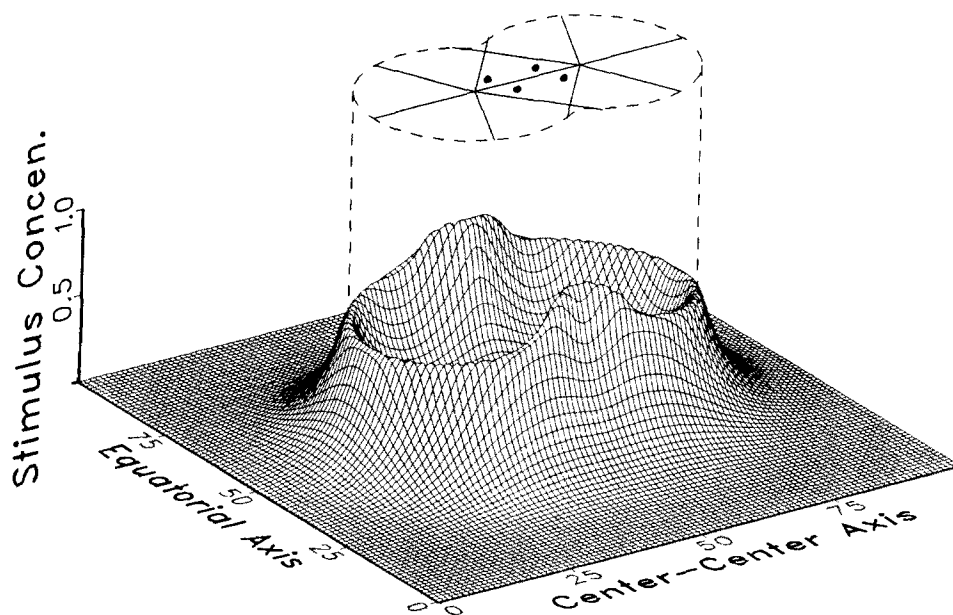
Figure 5. Pattern of cortical stimulation in a fertilized sand dollar egg experimentally constricted before division. Using the actual dimensions of cells thus constricted and asters located as previously described (32), the model predicts that differentially higher levels of stimulation should occur in the region of the artificial constriction. A cleavage furrow actually forms and goes to completion in that constriction (32), as predicted. Shadow angle (*dots*), 45°.

ulus appears to move could, conceivably, be a reflection of a mixture of at least three types of movements: astral ray microtubule elongation, transport of materials along microtubules, and diffusion of stimulus free in the cytoplasm. In the cytoplasm of living cells, individual microtubules have been observed to elongate at mean rates of 3.5 ± 3.2 μm/min (35). Various types of particles have been observed to be transported along astral rays (mostly away from the cell surface toward the microtubule minus ends in the astral centers) at 9–79 μm/min (9, 44), although some particles and organelles undergo transport in the plus direction at equal rates (9, 6). Microtubule-associated protein 1C facilitates transport along microtubules at 75 ± 6.6 μm/min (24) toward the minus end of microtubules, whereas kinesin facilitates transport along microtubules at ~46.2 ± 2.4 μm/min (17) toward the plus end of microtubules. The diffusion characteristics of the stimulus cannot be predicted at this time because no information is available about the class of molecule that is involved. The stimulus released by the astral rays might be an ion (e.g., Ca^{2+}), a small molecule (e.g., inositol trisphosphate), or a protein (e.g., calmodulin or myosin light chain kinase). Although the diffusion of ions or small molecules through cytoplasm near the cortex/plasma membrane may occur at rates comparable with those in solutions in vitro, diffusion of proteins in the cytoplasm of living cells occurs at rates not dependent on their molecular masses (range of 12–440 kD) (18). For these reasons, the model proposed includes a variable for diffusion of the stimulus, allowing insertion of actual rates when realistic data become available.

One method of testing the model is to determine its ability to predict the location of the cleavage furrow in cells containing an eccentrically located mitotic apparatus. For example, in very large cells the mitotic apparatus must be near the surface to initiate cytokinesis. The furrow forms as a crescent-shaped band that lengthens and deepens. This arises in fertilized eggs of amphibians, reptiles, fish, and birds (15), where the aster–aster axis is parallel to an essentially planar or only slightly curved plasma membrane/cortex. The model presented here correctly predicts the differential stimulation of

a linear band of cortex in such cells (Fig. 3). Translation into three dimensions generates a band of differential stimulation in the equatorial zone closest to the astral pair. The model can accommodate, but does not require, a role for the plasma membrane as a reflective barrier to the diffusion of stimulus in this and all other cellular shapes. In very large cells containing one eccentrically situated mitotic apparatus, a furrow begins and progressively lengthens, deepens, and becomes self-propagating. Whether such a furrow cleaves the cell completely (fertilized amphibian eggs) or only incompletely (fertilized eggs of elasmobranchs, bony fishes, birds, and reptiles) may be determined by the degree to which cytoplasmic inclusions, such as yolk, impede its progress (15).

Another test is to determine what the model predicts for cells containing more than one mitotic apparatus. Fertilized eggs of insects, such as *Drosophila*, for example, display nuclear divisions initially not accompanied by cytokinesis (5, 19). However, after nuclei migrate to the cell surface and form multiple mitotic apparatuses, cleavage furrows form in three regions: between each astral pair connected by a spindle, between polar regions of unreleated asters, and between sides of unrelated asters. The plasma membrane/cortex presents equatorial zones to be stimulated in all of these cases. The model accounts for differential equatorial stimulation in the three cases because each pair of related and unrelated asters, if sufficiently close to one another, generates the zone of astral ray overlap required to stimulate differentially a band of cortex (Fig. 4). Does a shadow effect (Fig. 1) exist between nonrelated asters in such regions? We postulate that it does, functionally. Visualizations of astral ray distributions between nonrelated asters are not sufficient currently to determine whether a shadow exists structurally (for insects see reference 19, Fig. 6 *B*, Fig. 8, and journal cover). However, experimentally produced aster–aster interdigitations allow metaphase-like arrangements of chromosomes (and of particles; 23) and anaphase separation of the chromosomes, as described by Boveri and by Baltzer (3) and more recently by Mazia et al. (20). Taken together with data on astral ray distributions in normal insect embryos (19), this suggests that

2230

in such regions of aster–aster interaction a shadow region of astral rays may function in the manner described in Fig. 1, even in the absence of a spindle.

The model has been assessed not only for its ability to predict the location of furrows in normal cells (Figs. 2–4) but also for cells whose shapes have been altered before division to engender contrasting predictions from the equatorial stimulation theory and the polar stimulation theory. For example, when fertilized sand dollar eggs are constricted experimentally with glass loops to reduce their diameter at the equator from the normal 142 to 78–80 μm (generating an hourglass shape) and allowed to position their mitotic apparatus so as to straddle the constriction, the distance from each astral center to the nearest pole is increased, whereas the distance from each astral center to the (constricted) equator is decreased (32). Previous formulations of the equatorial stimulation theory (26, 30) predicted that a furrow would form at the constriction, whereas polar stimulation theories (45–47) predicted that no furrow would form at the constriction. When the experimentally produced altered cell shapes and aster placements were used in the current model, it predicted that a zone of differentially higher stimulation would occur at the base of the artificial constriction (Fig. 5), suggesting that a furrow should form there. The actual experimental result was that a furrow did form at the base of the constriction and cleaved the cell (32), a result inconsistent with polar stimulation but consistent with the equatorial stimulation theory and the model proposed here.

A final test of the model was performed using experimental data from a study in which fertilized sand dollar eggs were constrained before division into long cylindrical shapes (33). Polar stimulation theories (46, 47) deal with such cells inadequately, first, by modeling them as ellipsoids rather than as long cylinders with genuinely parallel sides and, second, by predicting that the mitotic apparatus can stimulate the formation of no furrow after stimulating the formation of one furrow (because the apparatus is postulated to have only a transient ability to cause furrowing). In contrast, equatorial stimulation theories, including the model proposed here, predict that a furrow will form between the asters in such cells anywhere the apparatus remains long enough to initiate furrowing ($\sim$1 min is usually sufficient [31]) and that the astral pair remains continuously active in its ability to stimulate furrowing. This theory therefore predicts the formation of multiple furrows if the apparatus is moved along the cell at time intervals. The model proposed here predicts that a band of differentially higher stimulation will form at any equatorial zone determined by the position of the astral pair in such cylindrical cells (Fig. 6). Such a stimulation pattern would be created at each new location as the astral pair is moved intermittently and therefore predicts the formation of a temporal sequence of furrows in a single long cell, as observed experimentally (for review see 30).

A model suggesting that astral rays release stimulus from their ends will not generate differential equatorial stimulation in spherical cells if rays are of equal lengths (data not shown). However, the model proposed here can yield such equatorial stimulation in spherical cells because of three specific features. First, astral rays grow to fill available space, consistent with observed behavior in normal and manipulated cells (13, 16, 36, 39, 41). Second, stimulus is released only from astral ray ends, irrespective of ray length. Actions of diffusion and decay are postulated to begin only after stimulus is released at each such site (Fig. 1), consistent with the ability of astral rays to transport material along their length (9, 44). And, third, a shadow is required for differential stimulation in the equatorial zone. The model therefore is similar to one considered by Asnes and Schroeder (2) (see their Fig. 8, case c) but, unlike their model, it does not require that the ends of the astral microtubules touch the cortex. Termination of astral rays near the cortex allows the diffusing stimulus to reach it.

Earlier computer models to account for cytokinesis (45, 46) provoked profitable discussions of alternatives more compatible with experimental results (30). We hope that the model proposed here will be similarly provocative. Its program is available.
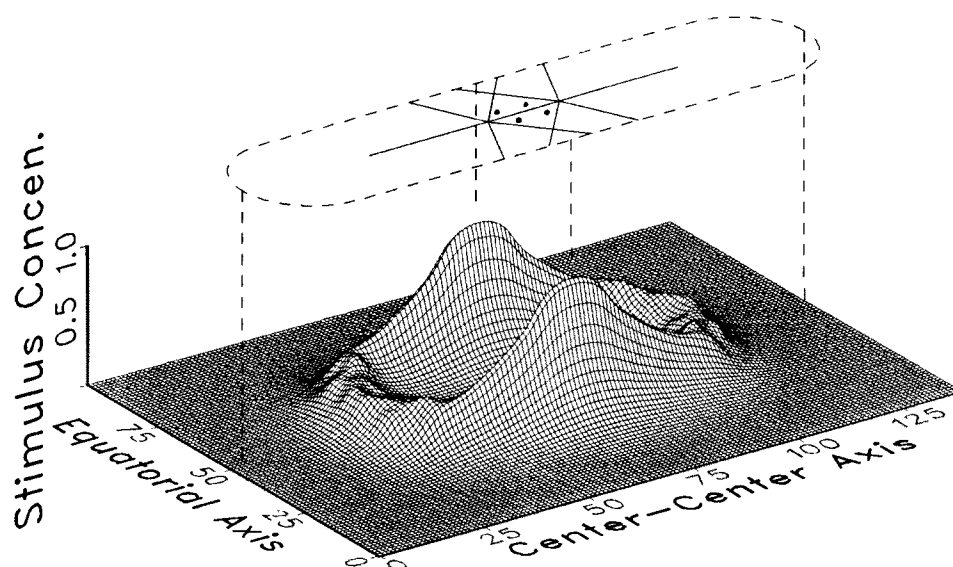
Figure 6. Pattern of cortical stimulation in a fertilized sand dollar egg experimentally constrained into a cylindrical shape before division. Using the actual dimensions of cells thus constrained and asters located as previously described (33), the model predicts that differentially higher levels of stimulation should occur in the equatorial region between the two asters, in a band encircling the cylinder. A cleavage furrow actually forms and goes to completion in that region (33) as predicted. Shadow angle (*dots*), 45°.

References

1. Armas-Portela, R., N. Paweletz, H.-P. Zimmermann, and S. Ghosh. 1988. Microtubule rearrangements during mitosis in multinucleate cells. *Cell Motil. Cytoskeleton.* 9:254–263.
2. Asnes, C. F., and T. E. Schroeder. 1979. Cell cleavage: ultrastructural evidence against equatorial stimulation by aster microtubules. *Exp. Cell Res.* 122:327–338.
3. Baltzer, F. 1967. Theodor Boveri: Life and Work of a Great Biologist. D. Rudnick, translator. University of Calif. Press, Berkeley, CA. 165 pp.
4. Bray, D., and J. G. White. 1988. Cortical flow in animal cells. *Science (Wash. DC).* 239:883–888.
5. Campos-Ortega, J. A., and V. Hartenstein. 1985. The Embryonic Development of *Drosophila melanogaster.* Springer-Verlag New York Inc., New York. 227 pp.
6. Dabora, S. L., and M. P. Sheetz. 1988. Cultured cell extracts support organelle movement on microtubules *in vitro. Cell Motil. Cytoskeleton.* 10:482–495.
7. Dan, K. 1988. Mechanism of equal cleavage of sea urchin egg: transposition from astral mechanism to constricting mechanism. *Zool. Sci. (Tokyo).* 5:507–517.
8. Gorbsky, G. J., P. J. Sammak, and G. G. Borisy. 1987. Chromosomes move poleward in anaphase along stationary microtubules that coordinately disassemble from their kinetochore ends. *J. Cell. Biol.* 104:9–18.
9. Hamaguchi, M. S., Y. Hamaguchi, and Y. Hiramoto. 1986. Microinjected polystyrene beads move along astral rays in sand dollar eggs. *Dev. Growth & Differ.* 28:461–470.
10. Hamaguchi, Y. 1975. Microinjection of colchicine into sea urchin eggs. *Dev. Growth & Differ.* 17:111–117.
11. Harris, A. K., and S. L. Gewalt. 1988. Simulation testing of mechanisms for inducing the formation of the contractile ring in cytokinesis. *J. Cell Biol.* 109:2215–2223.
12. Harris, P. 1988. Metaphase to anaphase transition of sea urchin eggs examined in caffeine-induced monasters. *Zool. Sci. (Tokyo).* 5:639–644.
13. Harris, P., M. Osborn, and K. Weber. 1980. Distribution of tubulin-containing structures in the egg of the sea urchin *Strongylocentrotus purpuratus* from fertilization through first cleavage. *J. Cell Biol.* 84:668–679.
14. Hiramoto, Y. 1956. Cell division without mitotic apparatus in sea urchin eggs. *Exp. Cell Res.* 11:630–636.
15. Hopper, A. F., and N. H. Hart. 1985. Foundations of Animal Development. 2nd. ed. Oxford University Press, New York. 595 pp.
16. Hyman, A. A., and J. G. White. 1987. Determination of cell division axes in the early embryogenesis of *Caenorhabditis elegans. J. Cell Biol.* 105:2123–2135.
17. Ingold, A. L., S. A. Cohn, and J. M. Scholey. 1988. Inhibition of kinesin-driven microtubule motility by monoclonal antibodies to kinesin heavy chains. *J. Cell Biol.* 107:2657–2667.
18. Jacobson, K., and J. Wojcieszyn. 1984. The translational mobility of substances within the cytoplasmic matrix. *Proc. Natl. Acad. Sci. USA.* 81:6747–6751.
19. Karr, T. L., and B. M. Alberts. 1986. Organization of the cytoskeleton in early *Drosophila* embryos. *J. Cell Biol.* 102:1494–1509.
20. Mazia, D., N. Paweletz, G. Sluder, and E.-M. Finze. 1981. Cooperation of kinetochores and pole in the establishment of monopolar mitotic apparatus. *Proc. Natl. Acad. Sci. USA.* 78:377–381.
21. Neighbors, B. W., R. C. Williams, Jr., and J. R. McIntosh. 1988. Localization of kinesin in cultured cells. *J. Cell Biol.* 106:1193–1204.
22. Ohta, K., M. Toriyama, S. Endo, and H. Sakai. 1988. Mitotic apparatus-associated 51-kD protein in mitosis of sea urchin eggs. *Zool. Sci.*

23. *(Tokyo).* 5:613–621.
23. Palazzo, R. E., J. B. Brawley, and L. I. Rebhun. 1988. Spontaneous aster formation in cytoplasmic extracts from eggs of the surf clam. *Zool. Sci. (Tokyo).* 5:603–611.
24. Paschal, B. M., H. S. Shpetner, and R. B. Vallee. 1987. MAP 1C is a microtubule-activated ATPase which translocates microtubules *in vitro* and has dynein-like properties. *J. Cell Biol.* 105:1273–1282.
25. Rappaport, R. 1961. Experiments concerning the cleavage stimulus in sand dollar eggs. *J. Exp. Zool.* 148:81–89.
26. Rappaport, R. 1971. Cytokinesis in animal cells. *Int. Rev. Cytol.* 31:169–213.
27. Rappaport, R. 1973. On the rate of movement of the cleavage stimulus in sand dollar eggs. *J. Exp. Zool.* 183:115–119.
28. Rappaport, R. 1981. Cleavage furrow establishment in cylindrical sand dollar eggs. *J. Exp. Zool.* 217:365–375.
29. Rappaport, R. 1982. Cytokinesis: the effect of initial distance between the mitotic apparatus and surface on the rate of subsequent cleavage furrow progress. *J. Exp. Zool.* 221:399–403.
30. Rappaport, R. 1986. Establishment of the mechanism of cytokinesis in animal cells. *Int. Rev. Cytol.* 105:245–281.
31. Rappaport, R., and R. P. Ebstein. 1965. Duration of stimulus and latent periods preceding furrow formation in sand dollar eggs. *J. Exp. Zool.* 158:373–382.
32. Rappaport, R., and B. N. Rappaport. 1984. Division of constricted and urethane-treated sand dollar eggs: a test of the polar stimulation hypothesis. *J. Exp. Zool.* 231:81–92.
33. Rappaport, R., and B. N. Rappaport. 1985. Surface contractile activity associated with isolated asters in cylindrical sand dollar eggs. *J. Exp. Zool.* 235:217–226.
34. Rieder, C. L., E. A. Davison, L. C. W. Jensen, L. Cassimeris, and E. D. Salmon. 1986. Oscillatory movements of monooriented chromosomes and their position relative to the spindle pole result from the ejection properties of the aster and half spindle. *J. Cell Biol.* 103:581–591.
35. Sammak, P. J., and G. G. Borisy. 1988. Direct observation of microtubule dynamics in living cells. *Nature (Lond.).* 332:724–726.
36. Sawada, T., and G. Schatten. 1988. Microtubules in ascidian eggs during meiosis, fertilization, and mitosis. *Cell Motil. Cytoskeleton.* 9:219–230.
37. Saxton, W. M., and J. R. McIntosh. 1987. Interzone microtubule behavior in late anaphase and telophase spindles. *J. Cell Biol.* 105:875–886.
38. Schatten G., C. Simerly, D. J. Asai, E. Szöke, P. Cooke, and H. Schatten. 1988. Acetylated α-tubulin in microtubules during mouse fertilization and early development. *Dev. Biol.* 130:74–86.
39. Schroeder, T. E. 1987. Fourth cleavage of sea urchin blastomeres: microtubule patterns and myosin localization in equal and unequal cell divisions. *Dev. Biol.* 124:9–22.
40. Sluder, G., and D. A. Begg. 1983. Control mechanisms of the cell cycle: role of the spatial arrangement of spindle components in the timing of mitotic events. *J. Cell Biol.* 97:877–886.
41. Spurck, T. P., and J. D. Pickett-Heaps. 1987. On the mechanism of anaphase A: evidence that ATP is needed for microtubule disassembly and not generation of polewards force. *J. Cell Biol.* 105:1691–1705.
42. Strome, S., and D. P. Hill. 1988. Early embryogenesis in *Caenorhabditis elegans:* the cytoskeleton and spatial organization of the zygote. *Bioessays.* 8:145–149.
43. Tanford, C. 1961. Physical Chemistry of Macromolecules. John Wiley & Sons Inc., New York. 710 pp.
44. Wadsworth, P. 1987. Microinjected carboxylated beads move predominantly poleward in sea urchin eggs. *Cell Motil. Cytoskeleton.* 8:293–301.
45. White, J. G. 1985. The astral relaxation theory of cytokinesis revisited. *Bioessays* 2:267–272.
46. White, J. G., and G. G. Borisy. 1983. On the mechanisms of cytokinesis in animal cells. *J. Theor. Biol.* 101:289–316.
47. White, J. G., and A. A. Hyman. 1987. On the implications of laterally mobile cortical tension elements for cytokinesis. *In* Biomechanics of Cell Division. N. Akkas, editor. Plenum Publishing Corp., New York. 79–96.
48. Yatsu, N. 1912. Observations and experiments on the ctenophore egg. I. The structure of the egg and experiments on cell division. *J. Coll. Sci. Imp. Univ. Tokyo.* 32(Art. 3):1–21.